# Stokes flow past compound multiphase drops: the case of completely engulfed drops/bubbles

By S. S. SADHAL and H. N. OGUZ

Department of Mechanical Engineering, University of Southern California,
Los Angeles, CA 90089-1453, USA

In this paper the translatory motion of a compound drop is examined in detail for low-Reynolds-number flow. The compound drop, consisting of a liquid drop or a gas bubble completely coated by another liquid, moves in a third immiscible fluid. An exact solution for the flow field is found in the limit of small capillary numbers by approximating the two interfaces to be spherical. The solution is found for the general case of eccentric configuration with motion of the inner sphere relative to the outer together with the motion of the system in the continuous phase. The results show that the viscous forces tend to move the inner-fluid sphere towards the front stagnation point of the compound drop. For equilibrium of the inner sphere with respect to the outer there must, therefore, be a body force towards the front. This can only be achieved with the necessary condition that there be a buoyant force on the inner sphere, opposite to that of the compound drop in the continuous phase. For a given set of fluids, two or four equilibrium configurations may be found. Of these only one or two, respectively, are stable. The others are unstable. For the special case of concentric configuration, the equilibrium is always metastable.

## 1. Introduction

In this paper we examine the fluid dynamics associated with a compound drop consisting of a drop or a bubble completely engulfed by a finite amount of another immiscible liquid. In particular, we investigate the translatory motion of such compound drops in a distinct third fluid for the general case when the spherical interfaces are eccentric (see figure 1). While the subject of compound drops was studied by Chambers & Kopac and Kopac & Chambers as early as 1937, it is only in the last two decades that it has emerged as a separate entity. The recent interest has been aroused by applications such as direct-contact heat exchange (Sideman & Moalem-Maron 1982) and membrane technology. The concept of coating drops and bubbles with liquid membranes has received recent attention concerning application in separation processes. Of particular interest in this regard is the area of artificial blood oxygenation (Li & Asher 1973). Direct-contact heat exchange is achieved by passing drops of one liquid through another immiscible liquid. If the drop liquid undergoes evaporation we have compound drops while the liquid and its vapour are both present. Similarly a vapour may be bubbled through an immiscible liquid. While the vapour is condensing compound drops will be formed. Although there have been a large number of experimental studies dealing with the translation of compound drops in relation to heat transfer (e.g. Mercier et al. 1974; Hayakawa & Shigeta 1974, Selecki & Gradon 1976, Tochitani et al. 1977; Mori 1978) few of these studies have addressed the theoretical fluid mechanics. The first thorough theoretical treatment
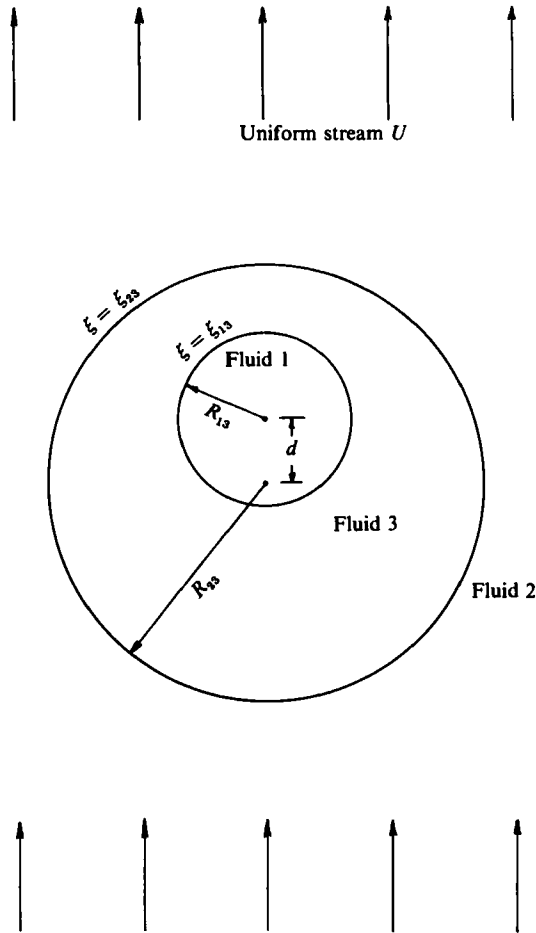
FIGURE 1. Schematic of the flow past a compound multiphase drop, in eccentric configuration. The uniform stream has a velocity $U$ relative to the outer spherical interface, which is fixed in the coordinate system. The inner spherical interface moves at a velocity $V$ relative to the outer interface.

of the statics of compound drops was carried out by Torza & Mason (1970). Recent theoretical studies on the dynamics include the analysis by Johnson & Sadhal (1983). They examined translating drops and bubbles partially coated with thin films by applying the lubrication-theory approximation.

The fluid motion resulting from the translation of fully encapsulated drops was examined by Rushton & Davies (1983) for the special case in which the encapsulating fluid is spherically concentric with the drop. The case of a melting ice particle coated with a layer of liquid water, translating in the atmosphere, has been treated by Rasmussen, Levizzani & Pruppacher (1982). They obtained an analytical solution for the spherically concentric case and a numerical solution for the eccentric cases. In addition to the flow problem, they treated the heat transfer for these configurations. In both of these analyses the inner sphere has been considered to be stationary with respect to the outer one. This assumption can be invalid in general as will be shown by a complete force balance on the inner sphere.

The thermally driven motion of eccentrically positioned gas bubbles within liquid

drops has been investigated by Shankar, Cole & Subramanian (1981) and Shankar & Subramanian (1983). Their principal result is a prediction of the bubble migration velocity in zero gravity for a prescribed temperature field on the drop surface. Some of the interest in this problem has been brought about by the potential application of glass processing in space.

With regard to oscillations of compound drops there have been numerous theoretical and experimental investigations. An extensive review of these studies, as well as those discussed above, is given by Johnson & Sadhal (1985).

The present investigation deals with the translation of an eccentrically encapsulated liquid drop in the limit of low Reynolds number. Also, the capillary numbers are taken to be small enough that the two interfaces may be assumed to be spherical. The exact solution in the limit of these approximations is found by using the bipolar coordinate system. This type of coordinate system was introduced by Jeffery (1912) and was used for Stokes flow past two spheres by Stimson & Jeffery (1926). It has subsequently been used by several authors for problems involving two spheres, or for a sphere near a plane. In particular, such problems involving solid spheres have been attacked by O'Neill (1964), Goren & O'Neill (1971) and Lee & Leal (1980). The more complex problems concerning the translation of two fluid spheres have been solved by Rushton & Davies (1973, 1978) and by Haber, Hetsroni & Solan (1973). The problem of the thermocapillary migration of a gas bubble normal to a plane surface has been treated by Meyyappan, Wilcox & Subramanian (1981) and Sadhal (1983).

In the next section we define the problem and derive its analytical solution.

## 2. Analysis

### 2.1. *Statement of problem*

We consider a liquid drop (or gas bubble) surrounded by a finite amount of liquid, forming a compound drop. This compound drop lies in a uniform stream of velocity $U$ moving parallel to the line of centres of the two spherical interfaces. Here the different phases are referred to as fluid 1, fluid 2 and fluid 3 as shown in figure 1. In the limit of large interfacial tension forces as compared with the viscous forces, the 2–3 interface is taken to be fixed in a spherical shape with tangential mobility. The 1–3 interface is also taken to be a sphere with tangential mobility, but it has translatory velocity $V$ parallel to the line of centres. The velocity of translation is determined by the total force balance on the inner sphere.

The governing equations in the limit of Stokes flow are as follows:

$$\left.\begin{array}{l} \mu_i \nabla^2 \boldsymbol{u}_i = \nabla p_i, \\ \nabla \cdot \boldsymbol{u}_i = 0 \end{array}\right\} \quad (i = 1, 2, 3; \text{ no sum}), \tag{2.1}$$
$$\tag{2.2}$$

where the subscripts refer to the three fluid phases, $\boldsymbol{u}$ is the velocity, $p$ is the pressure and $\mu$ is the viscosity. The boundary and the interface conditions are as follows.

(i) *Uniform stream at infinity*:

$$\boldsymbol{u}_2 \to U\hat{\boldsymbol{z}} \quad \text{as } (r^2 + z^2)^{\frac{1}{2}} \to \infty, \tag{2.3}$$

where $\hat{\boldsymbol{z}}$ is a unit vector along the line of centres.

(ii) *Zero normal velocity at the outer interface*:

$$\boldsymbol{u}_2 \cdot \boldsymbol{n}_{23} = \boldsymbol{u}_3 \cdot \boldsymbol{n}_{23} = 0, \tag{2.4}$$

where $\boldsymbol{n}_{23}$ is a unit normal at the 2–3 interface.

(iii) *Continuity of tangential velocity at the outer interface:*

$$\boldsymbol{u_2} \cdot \boldsymbol{t_{23}} = \boldsymbol{u_3} \cdot \boldsymbol{t_{23}}, \tag{2.5}$$

where $\boldsymbol{t_{23}}$ is the unit projection vector at the 2–3 interface.

(iv) *Continuity of shear stress at the outer interface:*

$$(\boldsymbol{\tau^{(2)}} - \boldsymbol{\tau^{(3)}}) : \boldsymbol{n_{23}} \, \boldsymbol{t_{23}} = 0, \tag{2.6}$$

where $\boldsymbol{\tau^{(i)}}$ represents the stress tensor in the respective fluids.

(v) *Continuity of normal velocity at the inner interface:*

$$\boldsymbol{u_1} \cdot \boldsymbol{n_{13}} = \boldsymbol{u_2} \cdot \boldsymbol{n_{13}} = V\hat{\boldsymbol{z}} \cdot \boldsymbol{n_{13}}, \tag{2.7}$$

where $\boldsymbol{n_{13}}$ is a unit normal vector at the 1–3 interface and $V$ is the unknown velocity of the inner spherical drop/bubble.

(vi) *Continuity of tangential velocity at the inner interface:*

$$(\boldsymbol{u_1} - \boldsymbol{u_3}) \cdot \boldsymbol{t_{13}} = 0, \tag{2.8}$$

where $\boldsymbol{t_{13}}$ is the unit projection vector at the 1–3 interface.

(vii) *Continuity of shear stress at the inner interface:*

$$(\boldsymbol{\tau^{(1)}} - \boldsymbol{\tau^{(3)}}) : \boldsymbol{n_{13}} \, \boldsymbol{t_{13}} = 0. \tag{2.9}$$

(viii) *Finite velocity in phase* 1:

$$\boldsymbol{u_1} < \infty. \tag{2.10}$$

With these boundary and interface conditions, the problem is fully defined. The normal-stress condition at both the interfaces is satisfied in the limit of very large surface-tension forces. An exact solution for this problem can be obtained by the use of the bipolar coordinate system. This system allows us to identify each interface by specifying constant values of one of the coordinates.

## 2.2. *The bipolar coordinate system*

By carrying out the transformation

$$z = \frac{c \sinh \xi}{\cosh \xi - \cos \eta}, \quad r = \frac{c \sin \eta}{\cosh \xi - \cos \eta} \tag{2.11}$$

we establish the $(\xi, \eta)$-coordinate system. In this system constant values of $\xi$ identify non-intersecting eccentric spheres. We identify the 1–3 interface by $\xi = \xi_{13}$ and the 2–3 interface by $\xi = \xi_{23}$. The radii of the interfaces are given by

$$R_{13} = \frac{c}{\sinh \xi_{13}}, \quad R_{23} = \frac{c}{\sinh \xi_{23}}. \tag{2.12}$$

Here $c$ is one half the distance between the points defined by $\xi \to \infty$ and $\xi \to -\infty$ on the $z$-axis. The distance between the centres may be expressed as

$$d = R_{23} [\cosh \xi_{23} - R \cosh \xi_{13}], \tag{2.13}$$

where

$$R = R_{13}/R_{23}. \tag{2.14}$$

With a little algebra we obtain the following forms for $\xi_{13}$ and $\xi_{23}$ in terms of $R$ and $d$:

$$\xi_{13} = \cosh^{-1}\left[ \frac{1 - R^2 - (d/R_{23})^2}{2(d/R_{23})R} \right]; \tag{2.15}$$

and

$$\xi_{23} = \cosh^{-1}\left[ \frac{1 - R^2 + (d/R_{23})^2}{2(d/R_{23})R} \right]. \tag{2.16}$$

With specified values of $R$ and $d/R_{23}$ the shape is fully defined. The dimensions can be further defined by specifying $c$ or either one of the radii. We define the eccentricity as

$$\epsilon = \frac{d}{R_{23} - R_{13}}.$$ (2.17)

At this point it is convenient to cast the problem in terms of the Stokes stream function. By expressing the velocity components as

$$(u_\xi^{(i)}, u_\eta^{(i)}) = \frac{(\cosh \xi - \cos \eta)^2}{c^2 \sin \eta} \left( \frac{\partial \psi_i}{\partial \eta}, -\frac{\partial \psi_i}{\partial \xi} \right) \quad (i = 1, 2, 3),$$ (2.18)

the continuity equation is identically satisfied. The momentum equation (2.1) is satisfied by $L_{-1}^2(\psi_i) = 0$ ($i = 1, 2, 3$) where $L_{-1}$ is the axisymmetric Stokes operator. In bipolar coordinates it is given by

$$L_{-1} = \frac{\sin \eta \, (\cosh \xi - \cos \eta)}{c^2} \left\{ \frac{\partial}{\partial \xi} \left[ \frac{\cosh \xi - \cos \eta}{\sin \eta} \right] \frac{\partial}{\partial \xi} + \frac{\partial}{\partial \eta} \left[ \frac{\cosh \xi - \cos \eta}{\sin \eta} \right] \frac{\partial}{\partial \eta} \right\}.$$ (2.19)

The shear stresses for an incompressible Newtonian fluid may be written as

$$\tau_{\xi\eta}^{(i)} = \mu_i \, T(\psi_i) \quad (i = 1, 2, 3; \text{ no sum}),$$ (2.20)

where $T$ is the operator given by

$$T = \frac{1}{c^3} \left\{ \frac{\partial}{\partial \eta} \left[ \frac{(\cosh \xi - \cos \eta)^3}{\sin \eta} \right] \frac{\partial}{\partial \eta} - \frac{\partial}{\partial \xi} \left[ \frac{(\cosh \xi - \cosh \eta)^3}{\sin \eta} \right] \frac{\partial}{\partial \xi} \right\}.$$ (2.21)

The boundary and interface conditions (2.3)–(2.10) may now be expressed in terms of $\psi_i$ ($i = 1, 2, 3$). In the bipolar coordinate system we write them as

(i) $\psi_2 |_{\xi, \eta \to 0} = \frac{1}{2} U c^2 \dfrac{\sin^2 \eta}{(\cosh \xi - \cos \eta)^2};$ (2.22)

(ii) $\psi_2 |_{\xi = \xi_{23}} = \psi_3 |_{\xi = \xi_{23}} = 0;$ (2.23a, b)

(iii) $\left. \dfrac{\partial \psi_2}{\partial \xi} \right|_{\xi = \xi_{23}} = \left. \dfrac{\partial \psi_3}{\partial \xi} \right|_{\xi = \xi_{23}};$ (2.24)

(iv) $\mu_2 \, T(\psi_2) |_{\xi = \xi_{23}} = \mu_3 T(\psi_3) |_{\xi = \xi_{23}};$ (2.25)

(v) $\psi_1 |_{\xi = \xi_{13}} = \psi_3 |_{\xi = \xi_{13}} = \frac{1}{2} V c^2 \dfrac{\sin^2 \eta}{(\cosh \xi_{13} - \cos \eta)^2};$ (2.26a, b)

(vi) $\left. \dfrac{\partial \psi_1}{\partial \xi} \right|_{\xi = \xi_{13}} = \left. \dfrac{\partial \psi_3}{\partial \xi} \right|_{\xi = \xi_{13}};$ (2.27)

(vii) $\mu_1 \, T(\psi_1) |_{\xi = \xi_{13}} = \mu_3 \, T(\psi_3) |_{\xi = \xi_{13}};$ (2.28)

(viii) $\psi_1 |_{\xi \to \infty} < \infty.$ (2.29)

## 2.3. *Solution*

We need to find a solution for Stokes equation $L_{-1}^2(\psi_i) = 0$ satisfying the boundary/interface conditions (2.22)–(2.29). In bipolar coordinates, the separation of variables for $\psi_i$ is not possible in the usual manner. However, by following Stimson & Jeffery (1926) we may write the solution in the following separable form:

$$\psi_i(\xi, \eta) = (\cosh \xi - \cosh \eta)^{-\frac{3}{2}} \sum_{n=0}^{\infty} \Xi_n^{(i)}(\xi) \, C_{n+1}^{-\frac{1}{2}}(\cos \eta),$$ (2.30)

where $C_{n+1}^{-\frac{1}{2}}(\ )$ is the Gegenbauer polynomial of order $(n+1)$ and degree $-\frac{1}{2}$. The general solution for $\Xi_n^{(i)}(\xi)$ is

$$\Xi_n^{(i)}(\xi) = A_n^{*(i)} \cosh\,(n-\tfrac{1}{2})\,\xi + B_n^{*(i)} \sinh\,(n-\tfrac{1}{2})\,\xi$$
$$+ C_n^{*(i)} \cosh\,(n+\tfrac{3}{2})\,\xi + D_n^{*(i)} \sinh\,(n+\tfrac{3}{2})\xi, \quad (2.31)$$

where $A_n^{*(i)}$, $B_n^{*(i)}$, $C_n^{*(i)}$ and $D_n^{*(i)}$ represent 12 integration constants.

We select solutions satisfying (2.22), (2.23), (2.26$a$), (2.29) to be of the following special forms:

$$\Xi_n^{(1)}(\xi) = V\frac{n(n+1)}{2\sqrt{2}}\left[\frac{e^{(n-\frac{1}{2})\xi}}{n-\frac{1}{2}} - \frac{e^{-(n+\frac{3}{2})\xi}}{n+\frac{3}{2}}\right] + B_n\left[e^{-(n-\frac{1}{2})\,(\xi-\xi_{13})} - e^{-(n+\frac{3}{2})\,(\xi-\xi_{13})}\right]; \qquad (2.32)$$

$$\Xi_n^{(2)}(\xi) = U\frac{n(n+1)}{2\sqrt{2}}\left[\left(\frac{e^{-(n-\frac{1}{2})\xi}}{n-\frac{1}{2}} - \frac{e^{-(n+\frac{3}{2})\xi}}{n+\frac{3}{2}}\right)\right.$$
$$\left. - \left(\frac{e^{(n-\frac{1}{2})\,(\xi-2\xi_{23})}}{n-\frac{1}{2}} - \frac{e^{(n+\frac{3}{2})\,(\xi-2\xi_{23})}}{n+\frac{3}{2}}\right)\right] + A_n\left[e^{(n-\frac{1}{2})\,(\xi-\xi_{23})} - e^{(n+\frac{3}{2})\,(\xi-\xi_{23})}\right]; \quad (2.33)$$

$$\Xi_n^{(3)}(\xi) = C_n \sinh\,[(n-\tfrac{1}{2})\,(\xi-\xi_{23})] + D_n \sinh\,[(n+\tfrac{3}{2})\,(\xi-\xi_{23})]$$
$$+ E_n\left\{\cosh\,[(n-\tfrac{1}{2})\,(\xi-\xi_{23})] - \cosh\,[(n+\tfrac{3}{2})\,(\xi-\xi_{23})]\right\}. \quad (2.34)$$

In satisfying (2.22) and (2.26), the following identity is made use of:

$$\frac{\sin^2\eta}{(\cosh\xi-\cos\eta)^{\frac{3}{2}}} = \sum_{n=0}^{\infty}\frac{n(n+1)}{2\sqrt{2}}\left[\frac{e^{-(n-\frac{1}{2})\xi}}{n-\frac{1}{2}} - \frac{e^{-(n+\frac{3}{2})\xi}}{n+\frac{3}{2}}\right]C_{n+1}^{-\frac{1}{2}}(\cos\eta). \qquad (2.35)$$

The constants $A_n$, $B_n$, $C_n$, $D_n$ and $E_n$ are to be determined by the remaining boundary conditions (2.24), (2.25), (2.26$b$), (2.27), (2.28). These constants are given in Appendix A.

With all the boundary and interface conditions satisfied the solution is formally complete. However, the velocity of the inner sphere and that of the uniform stream need to be specified. This is done in the next section by requiring the total force on each spherical interface to be zero.

## 3. Translational velocities and the drag force

The viscous drag on each sphere may be calculated by a formula given by Stimson & Jeffery (1926). For a given set of radii and an eccentricity, each viscous drag is a linear function of $U$ and $V$. These forces are balanced by the buoyant forces. By having a total-force balance on each spherical interface, the following linear equations are obtained (see Appendix B):

inner sphere:
$$\tfrac{4}{3}\pi R_{13}^3(\rho_1-\rho_3)\,g = \alpha U + \beta V = f_D; \qquad (3.1)$$

outer sphere:
$$\tfrac{4}{3}\pi[R_{13}^3\rho_1 + (R_{23}^3 - R_{13}^3)\rho_3 - R_{23}^3\rho_2]\,g = \gamma U + \delta V = F_D; \qquad (3.2)$$

where $f_D$ and $F_D$ represent the forces of viscous drag on the inner and outer spheres, respectively. The constants $\alpha$, $\beta$, $\gamma$ and $\delta$ are given in Appendix B. By solving the set (3.1), (3.2) we obtain $U$ and $V$ in the following dimensionless forms;

$$U^* = \frac{U}{R_{23}^2 g\rho_2/\mu_2} = \frac{f_D^*\delta^* - F_D^*\beta^*}{\alpha^*\delta^* - \beta^*\gamma^*}, \qquad (3.3)$$
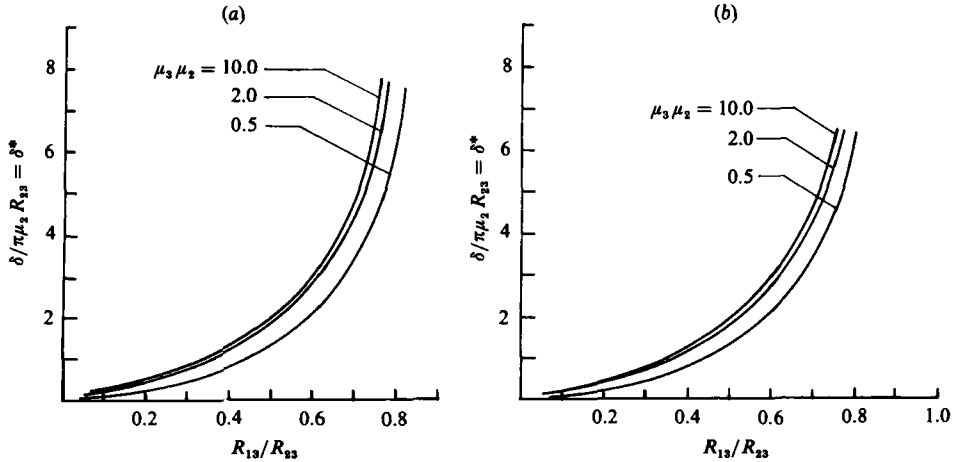
FIGURE 2. The contribution to the total drag force as function of the radius ratio for given eccentricities and viscosity ratios, $\mu_1 = \mu_2$. (a) $\epsilon = 0.05$; (b) 0.5.

and

$$V^* = \frac{V}{R_{23}^2 g \rho_2 / \mu_2} = \frac{F_D^* \alpha^* - f_D^* \gamma^*}{\alpha^* \delta^* - \beta^* \gamma^*} \tag{3.4}$$

where

$$(\alpha^*, \beta^*, \gamma^*, \delta^*) = \frac{\alpha, \beta, \gamma, \delta}{\pi \mu_2 R_{23}}, \tag{3.5}$$

$$f_D^* = \frac{4}{3}\left(\frac{R_{13}}{R_{23}}\right)^3 \left(\frac{\rho_1}{\rho_2} - \frac{\rho_3}{\rho_2}\right), \tag{3.6}$$

and

$$F_D^* = \frac{4}{3}\left\{\left(\frac{R_{13}}{R_{23}}\right)^3 \left[\left(\frac{\rho_1}{\rho_2}\right) - \left(\frac{\rho_3}{\rho_2}\right)\right] + \left(\frac{\rho_3}{\rho_2} - 1\right)\right\}. \tag{3.7}$$

As we see above, the other dimensionless parameters may be selected as $\rho_1/\rho_2$, $\rho_3/\rho_2$, $\mu_3/\mu_2$, $\mu_1/\mu_2$ and $R_{23}/R_{13}$.

It must be recognized that the expression for $V$ is the instantaneous steady-state velocity and is valid only in the low-Reynolds-number approximation. In a given system, as the eccentricity changes with the motion of the inner sphere, its velocity changes. The present approximation will only allow slow changes in the velocity.

The numerical calculations of these results display some interesting features. For a given system of fluids with specified $\mu_i$, $\rho_i$, $i = 1, 2, 3$, and given volumes $V_1$ and $V_3$, it is found that $U$ changes very little with eccentricity. Therefore, its use as a scaling parameter for $V$ is quite appropriate. In general $V$ is non-zero, indicating that the relative motion of the inner sphere is necessary. If the condition that it be fixed is imposed then the total force on it may be non zero. The viscous force on it, as we see in (3.1), consists of two parts. One is the 'primary viscous force' which is the force when $V = 0$, and it is proportional to $U$. The other is the 'secondary viscous force' which is proportional to $V$. The motion of the inner sphere generates the secondary viscous force to overcome the net force that exists without the motion.

An examination of the total drag force $F_D$ shows that it has a strong dependence on the relative motion of the inner sphere. In figure 2 we show the contribution of $V$ towards $F_D$. The factor $\delta$ in (3.2) is plotted as a function of the radius ratio $R = R_{13}/R_{23}$ for various viscosity ratios and two different eccentricities. The force tends to become infinitely large as the fluid shell (fluid 3) becomes infinitesimally thin.
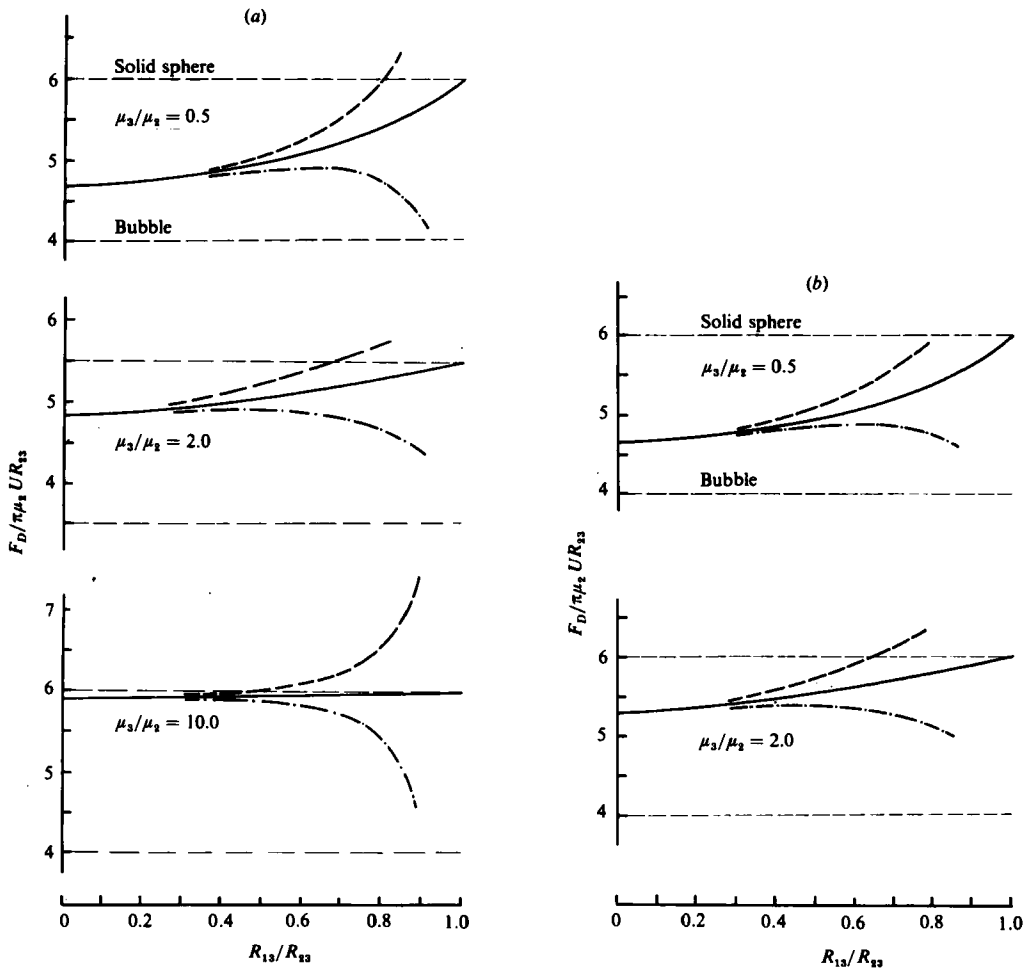
FIGURE 3. The total drag as a function of the radius ratio for various values of the viscosity ratios and inner sphere relative velocity; (a) $\epsilon = 0.05$, (b) 0.5. ----, $V/u = 0.1$; ——, 0; —·—, 0.1.

In figure 3 we plot $F_D$ as a function $R$ for various values of $V/U$ and two different eccentricities. We see that, with the inner-sphere motion opposite to the uniform stream, $F_D$ is higher than for $V = 0$. The drag is lower when inner-sphere motion is in the same direction as the uniform stream. The reason for such behaviour is the necessity of external forces on the inner sphere to maintain such motion involving arbitrarily chosen values of $V$.

The drag force $F_D$ for $V = 0$ varies between the bubble drag and the solid-sphere drag. It seems to have little dependence on $\epsilon$. As the fluid shell becomes very thin, the solid-sphere limit is observed. This is because the motion within the thin shell requires a strong shear stress. This stress should be matched by the outer fluid, which can afford only moderate stresses. Consequently, the motion within the shell must weaken. In the limit of very small thickness, the shell is practically motionless. This observation has been made for spherically symmetric cases by Rushton & Davies (1983).

While the drag force depends strongly on the inner-sphere motion, it must be understood that $V$ is a determinate quantity given by (3.4). The behaviour of $V$ as a function of the eccentricity for a given system is a matter of considerable interest
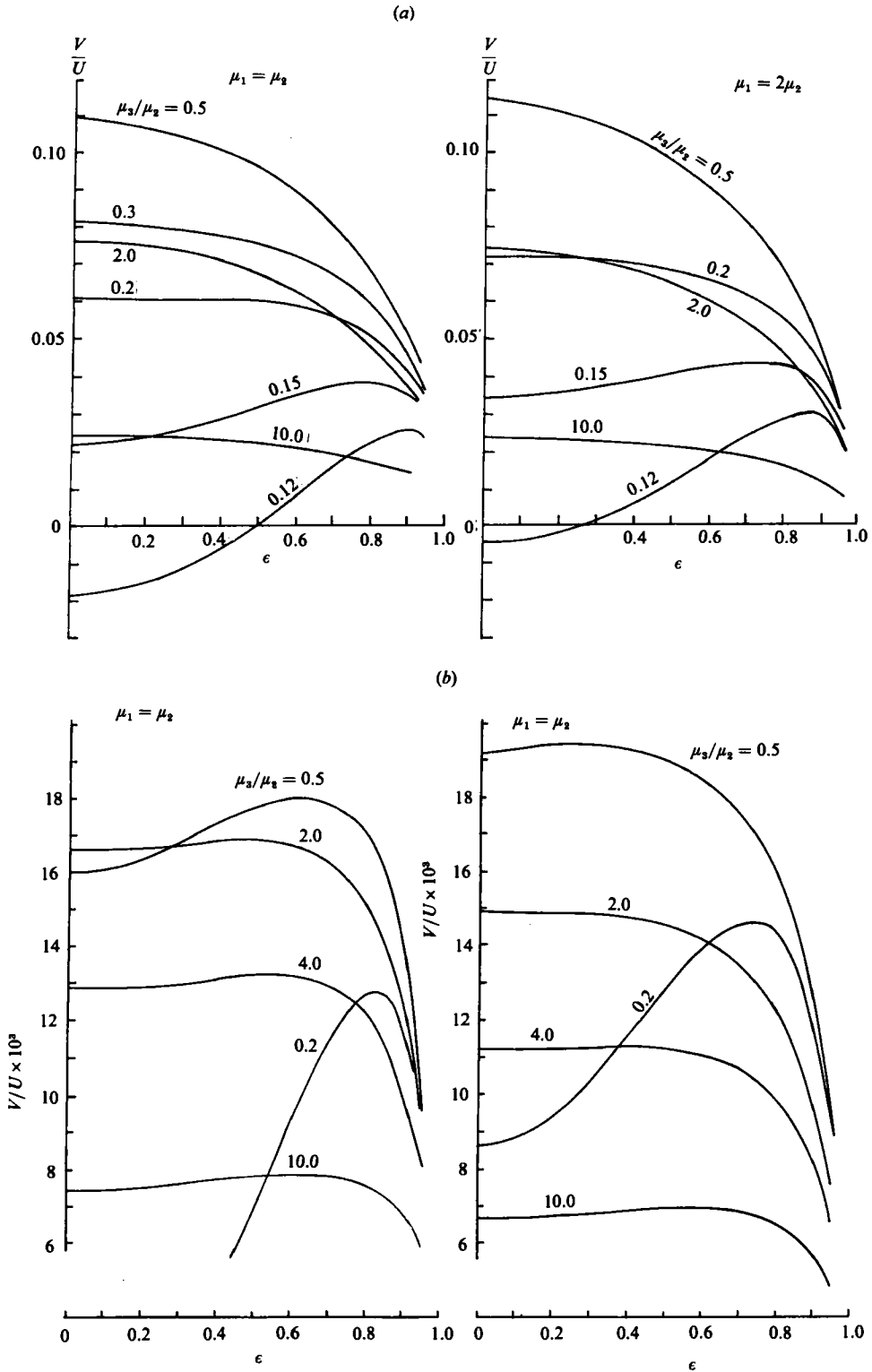
FIGURE 4. The inner-sphere relative velocity as a function of eccentricity. The system has a net upward buoyancy, $\rho_1 = \rho_2$, $\rho_3 = 0.8\rho_2$, and radius ratio of (a) 0.5 and (b) 0.8.
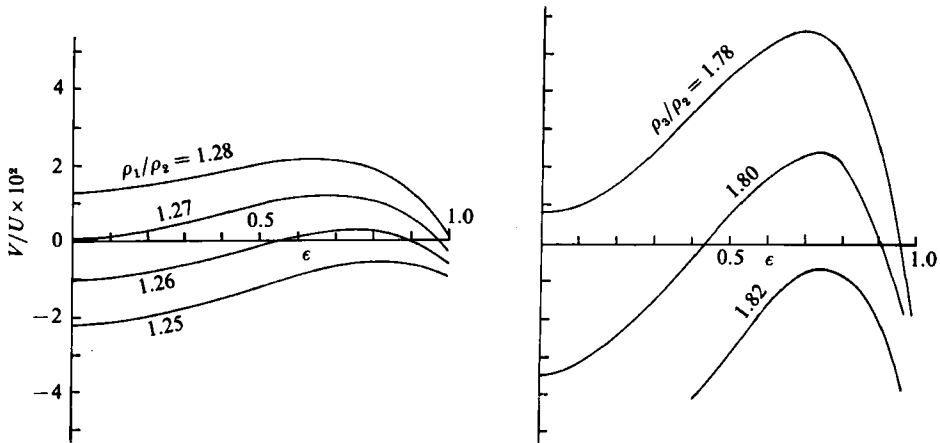
FIGURE 5. Relative velocity of the inner sphere as a function of the eccentricity for situations of high viscosity of phase 3, $R_{13}/R_{23} = 0.45$. In case (a) $\rho_3 = 0.8\rho_2$, $\mu_3 = 10\mu_2$, $\mu_1 = \mu_2$, the net buoyant force on the compound drop is upwards and in (b), $\mu_3 = 10\mu_2$, $\mu_1 = 0$, $\rho_1 = 0$, it is downwards. For both the cases there is the possibility of two equilibrium eccentricities.
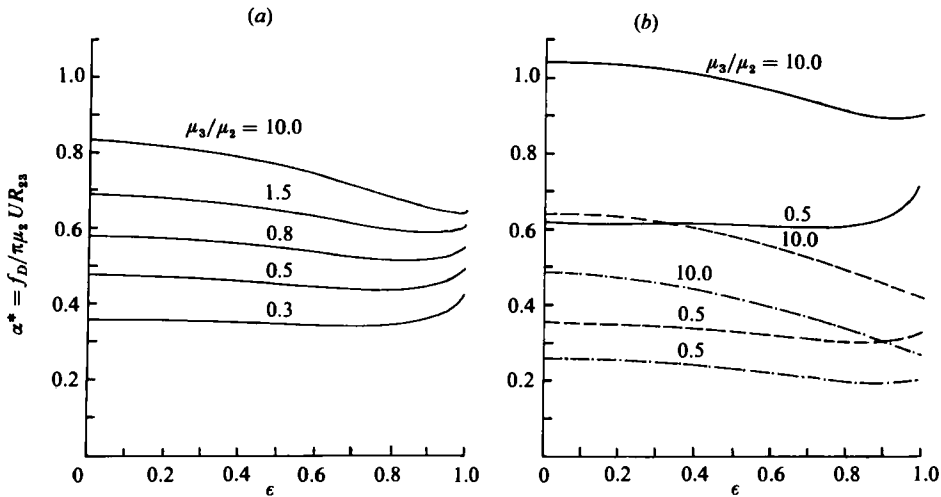


FIGURE 6. The force on the inner sphere as a function of eccentricity for $V = 0$, $\mu_1 = \mu_2$. (a) $R_{13}/R_{23} = 0.3$; (b) ——, $R_{13}/R_{23} = 0.35$; —---, 0.25; —·--, 0.20.

in understanding the behaviour of multiphase drops. In figure 4 (a, b) we plot $V/U$ versus the eccentricity $\epsilon$ for a range of the dimensionless parameters. We see from these plots that in most cases there is a weak relative motion of the inner sphere. These cases represent fluids of comparable densities and viscosities with a net downward buoyant force. When the buoyant force on the inner sphere exactly balances the primary viscous force, we have equilibrium of the inner sphere with respect to the outer. This is graphically represented by the points where the plot of $V/U$ versus $\epsilon$ intersects the horizontal axis. These points correspond to the specific eccentricities at which there is no motion of the inner sphere with respect to the outer (i.e. $V = 0$). In figure 5 we plot $V/U$ versus $\epsilon$ for large shell viscosities. We see that in many instances the equilibrium occurs for two different eccentricities. In general,

for each eccentricity there are two possible configurations: one with the inner sphere towards the front of the compound drop; the other towards the rear. The stability analysis in §4, however, shows that only one configuration for each equilibrium eccentricity is stable.

The primary drag force on the inner sphere (the term $\alpha$ in (3.1)) is plotted as a function of $\epsilon$ in figure 6. It represents monotonic behaviour in some cases but shows definite turning points in many instances, particularly for $R < 0.5$. Since this force is the viscous force when the inner sphere is fixed with respect to the outer, there must be an external opposite force to balance this out. The external force is usually the buoyancy, which may be represented by a horizontal straight line. At points where this line intersects the other curves we have equilibrium. Here again it is evident that there may be either one or two possible eccentricities for equilibrium. For a buoyant force completely outside the range of the primary drag force there will be no equilibrium.

The question of the stability of the various equilibrium configurations now arises. This is discussed next.

## 4. Stability analysis

The primary viscous force is always in a direction opposite to the flow of the uniform stream. Therefore, for the compound drop having a downward buoyant force $[\rho_1 V_1 + \rho_3 V_3 > \rho_2(V_1 + V_2)]$, the primary force on the inner sphere is downwards. This could be exactly balanced by an upward buoyant force provided $\rho_1 < \rho_3$. For a specific value of $\epsilon$, for which this balance takes place, there are two configurations possible. In one case the inner sphere is off-centre towards the front stagnation point and in another case it is towards the rear. In both cases the primary viscous drag is identical. Since the buoyant force is unaffected by the different positions, both of them represent equilibrium configurations. Let us examine the case in which the inner sphere is near the front. For this purpose we make a schematic plot of $V/U$ versus the position of the inner sphere with respect to the outer (see figure 7). Here the different curves represent variations in the buoyant forces and/or the viscosities. We see that increasing the eccentricity will give it a downward velocity and decreasing it will give it an upward velocity. This configuration is clearly a case of unstable equilibrium. For the case with the inner sphere towards the rear, a similar examination shows stable equilibrium. Hence, a compound drop set in motion with above-mentioned density requirements will reach a steady state with the inner sphere towards the rear. In the event that the system starts with the inner sphere towards the front with an eccentricity higher than the equilibrium case, the tendency would be to expel the inner sphere. With an initial eccentricity slightly less than the equilibrium case, the inner sphere will migrate from the front towards the rear until it reaches the stable equilibrium configuration.

For the opposite density requirements $[\rho_1 V_1 + \rho_3 V_3 < \rho_2(V_1 + V_2)$ and $\rho_3 < \rho_1]$, an unstable equilibrium results, with the inner sphere near the rear stagnation point. A stable equilibrium can be found near the front stagnation point. For a rising compound drop $[\rho_1 V_1 + \rho_3 V_3 < \rho_2(V_1 + V_2)]$ with upward buoyancy on the inner sphere ($\rho_1 < \rho_3$), no equilibrium can be found. Similarly with $\rho_1 V_1 + \rho_3 V_3 > \rho_2(V_1 + V_2)$ and $\rho_3 < \rho_1$ an equilibrium configuration cannot be found. In both instances the tendency would be to expel the inner sphere towards the front.

For the cases having two different eccentricities corresponding to $V = 0$ (see figure 5) there are four different equilibrium configurations; two near the front, and
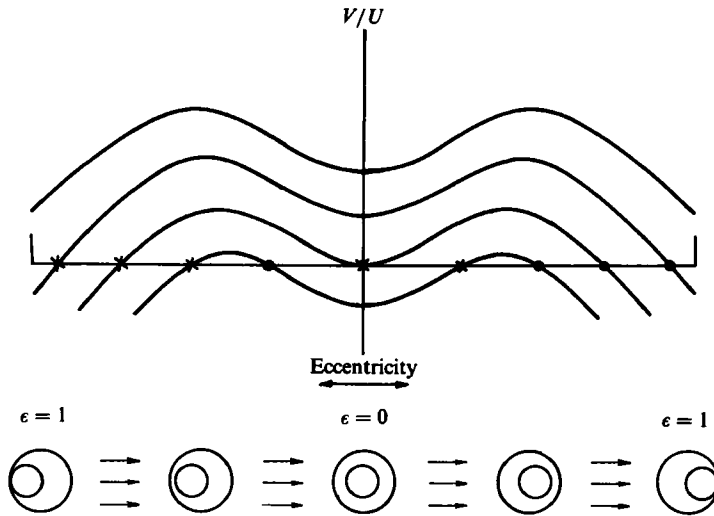
FIGURE 7. Schematic of the inner-sphere velocity as a function of its relative position. ●, stable equilibrium; ×, unstable equilibrium; ✖, metastable states.
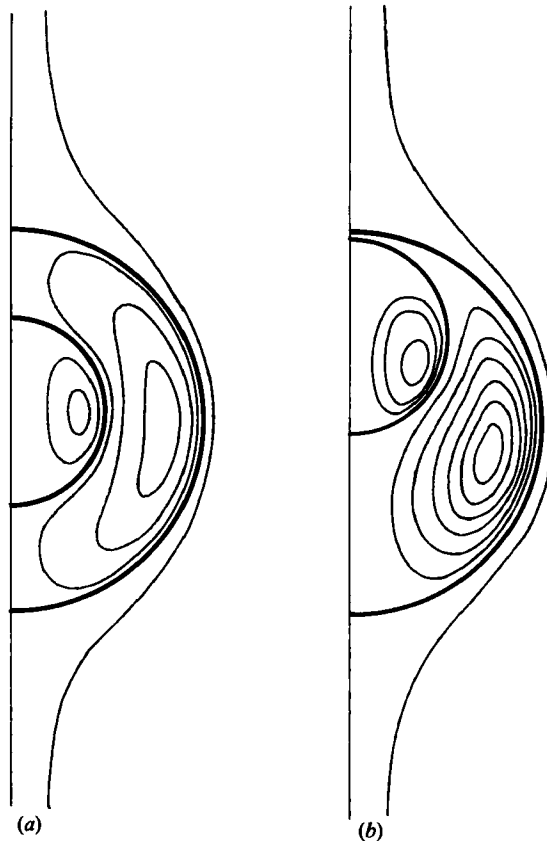


FIGURE 8. Flow streamlines for a radius ratio of 0.5 with eccentricities (a) 0.1 and (b) 0.9. $\mu_3 = 10\mu_2 = 10\mu_1$; $V = 0$.
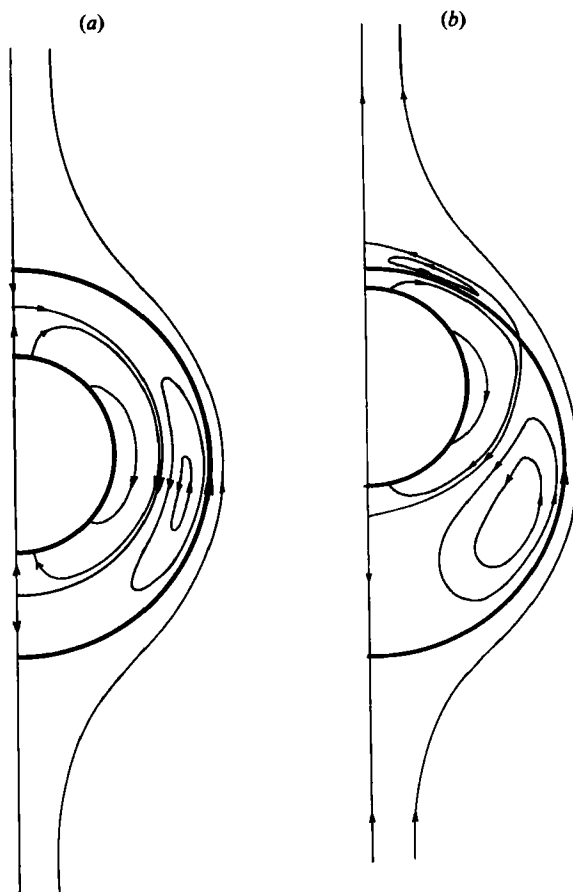
FIGURE 9. Double-vortex structure generated in the phase 3 fluid owing to motion of the inner-fluid sphere: (a) $\epsilon = 0.1$; (b) 0.8. $\mu_3 = 5\mu_1 = 5\mu_2$; $R = 0.5$; $V/U = 0.04$. For high eccentricity ($\epsilon = 0.8$) there is an additional vortex in phase 2 near the rear of the compound drop.

two near the rear. With the density conditions $\rho_1 V_1 + \rho_3 V_3 > \rho_2(V_1 + V_2)$ and $\rho_1 < \rho_3$, the equilibrium position with the higher eccentricity and inner sphere towards the rear is a stable one. Similarly, the one with the lower eccentricity and the inner sphere towards the front is also stable. The other two are unstable. The same type of argument applies to the cases $\rho_1 V_1 + \rho_3 V_3 < \rho_2(V_1 + V_2)$, $\rho_1 > \rho_3$. In this situation the higher-eccentricity configuration is stable towards the front and the lower towards the rear. These conclusions regarding the stability are evident from figure 7.

For the spherically symmetric case we can see that, when we balance out the body force and the viscous drag, the equilibrium state is a metastable one. Any disturbance from this state tends to move the inner sphere towards the front of the compound drop.

## 5. The flow field

The flow streamlines have been plotted for a variety of cases. In many instances they display rather fascinating flow patterns. In figure 8 we have the streamlines for two equilibrium situations. Here the flow pattern within the compound drop is as expected. There is considerable resemblance here to the flow field numerically

(a)                                          (b)
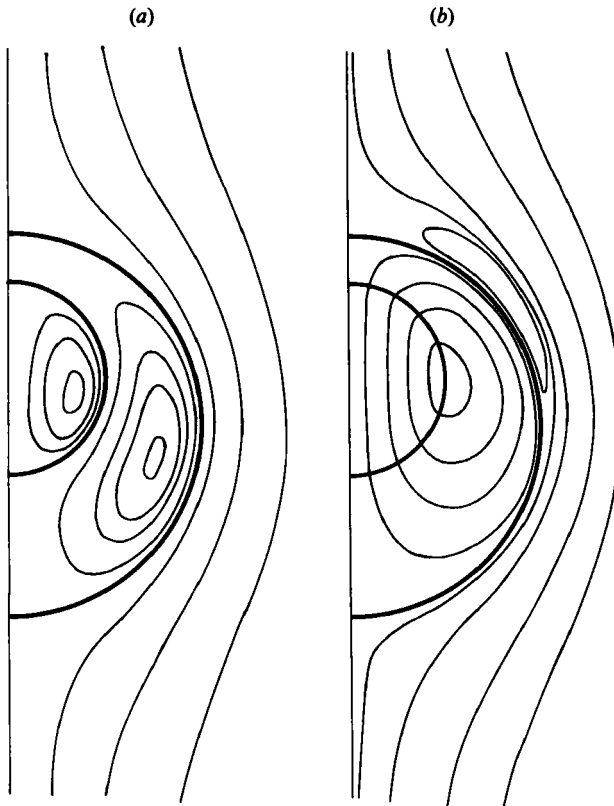


FIGURE 10. Comparison of the flow pattern with and without inner-sphere motion: (a) $V = 0$, (b) $V = 0.2U$. $\mu_3 = \mu_2 = 10\mu_1$; $R = 0.5$; $\epsilon = 0.5$. For sufficiently high viscosity in phase 3 the streamlines are completely reversed when the inner sphere moves in the same direction as the uniform stream.

obtained by Rasmussen *et al.* (1982) for melting ice particles. For situations in which the inner sphere moves with respect to the outer, we observe quite interesting double and triple-vortex structures in some cases. In figure 9 we have the inner sphere moving in the same direction as the uniform stream. In such cases the inner-sphere motion generates streamlines in the opposite direction to those generated by the uniform stream within the shell. Consequently we have a double-cell structure within the fluid shell as shown in figure 9(a). For larger eccentricities a small vortex is generated within the continuous phase (fluid 2) as observed in figure 9(b). This is particularly true if the shell fluid has relatively high viscosity. Additional demonstration of this behaviour is given in figure 10, where a comparison of the flow patterns with and without inner-sphere motion are given. For cases in which the inner sphere moves in a direction opposite to the uniform stream, the double-cell structure is not present. This is demonstrated by the comparisons in figures 10 and 11.

## 6. Concluding remarks

In the present analysis we have carried out a detailed theoretical study of the motion of compound two-fluid drops. This study is limited to situations of creeping flow with high surface-tension forces as compared with the viscous forces. We have only examined cases in which the compound drop consists of one fluid completely
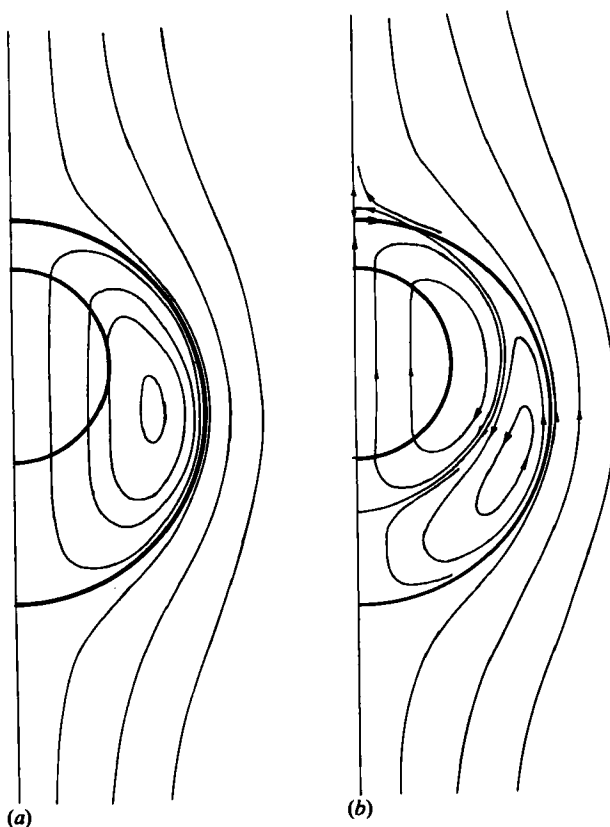
FIGURE 11. Comparison of flow fields for different directions of inner-sphere motion. (*a*) $V = -0.2U$; (*b*) $V = 0.2U$. The viscosities of the three fluids are of similar magnitude, $\mu_3 = 0.5\mu_2 = 0.5\mu_1$; $R = 0.5$, $\epsilon = 0.5$.

engulfing another. Through exact solutions in the Stokes-flow regime we have been able to acquire fundamental knowledge about the flow pattern and the dynamic stability of such three-fluid systems. While we have allowed large eccentricities in our solution, it is quite clear that in many instances we may have very large fluid pressures that would disallow the spherical-interfaces approximation. The question of deformation is currently under examination.

From the present analysis we draw some important conclusions about the behaviour of translating compound drops. For a compound drop of specified composition moving through a given fluid in a force field there would, in general, be relative motion between the two spherical surfaces. In some cases the net viscous force on the inner sphere would exactly balance the buoyant force without any relative motion. These are cases of equilibrium. In general we find either two or four equilibrium positions of the inner sphere. However, only one or two of these, respectively, are stable. The other are unstable. In the case of equilibrium for a spherically concentric case the behaviour is metastable. We also see that an equilibrium configuration is highly sensitive to small changes in the buoyant force on the inner sphere.

This work represents a fundamental advancement in relation to direct-contact heat/mass exchange and liquid-membrane technology. Also of interest in this context are cases in which the innermost fluid (fluid 1) experiences growth or collapse owing

to evaporation or condensation, respectively. The present analysis did not treat such cases. However, they are currently being examined. Our efforts are also being focused on situations in which we have compound drops with one fluid partially contacting the second. The heat/mass-transfer aspects of such systems are also under examination, both theoretically and experimentally.

## Appendix A

With the solution for the stream functions given by (2.20), (2.32)–(2.34) the unknown integration constants $A_n$, $B_n$, $C_n$, $D_n$ and $E_n$ may be obtained by satisfying the interface conditions (2.24), (2.25), (2.26$b$), (2.27), (2.28). These conditions lead to a set of $5 \times 5$ linear algebraic equations for these constants. The solution to this set yields the following:

$$A_n = (U A_n^{(1)} + V A_n^{(2)}) c^2; \tag{A 1}$$

$$B_n = (U B_n^{(1)} + V B_n^{(2)}) c^2; \tag{A 2}$$

$$C_n = (U C_n^{(1)} + V C_n^{(2)}) c^2; \tag{A 3}$$

$$D_n = (U D_n^{(1)} + V D_n^{(2)}) c^2; \tag{A 4}$$

$$E_n = (U E_n^{(1)} + V E_n^{(2)}) c^2; \tag{A 5}$$

where

$$E_n^{(1)} = -\frac{\mu_2}{2\mu_3} \left\{ \frac{n(n+1)}{2\sqrt{2}} \left[ e^{-(n-\frac{1}{2})\xi_{23}} - e^{-(n+\frac{3}{2})\xi_{23}} \right] + (n-\tfrac{1}{2}) C_n^{(1)} + (n+\tfrac{3}{2}) D_n^{(1)} \right\}, \tag{A 6}$$

$$E_n^{(2)} = -\frac{\mu_2}{2\mu_3} \left[ (n-\tfrac{1}{2}) C_n^{(2)} + (n+\tfrac{3}{2}) D_n^{(2)} \right], \tag{A 7}$$

$$A_n^{(1)} = \frac{\mu_3}{\mu_2} E_n^{(1)}, \tag{A 8}$$

$$A_n^{(2)} = \frac{\mu_3}{\mu_2} E_n^{(2)}, \tag{A 9}$$

$$B_n^{(1)} = \tfrac{1}{2}\{ C_n^{(1)}(n-\tfrac{1}{2}) \cosh\left[(n-\tfrac{1}{2})(\xi_{13}-\xi_{23})\right] + D_n^{(1)}(n+\tfrac{3}{2}) \cosh\left[(n+\tfrac{3}{2})(\xi_{13}-\xi_{23})\right]$$
$$+ E_n^{(1)} \{ (n-\tfrac{1}{2}) \sinh\left[(n-\tfrac{1}{2})(\xi_{13}-\xi_{23})\right] - (n+\tfrac{3}{2}) \sinh\left[(n+\tfrac{3}{2})(\xi_{13}-\xi_{23})\right]\}\}, \tag{A 10}$$

$$B_n^{(2)} = \frac{n(n+1)}{8\sqrt{2}} \left[ e^{-(n-\frac{1}{2})\xi_{13}} - e^{-(n+\frac{3}{2})\xi_{13}} \right] + C_n^{(2)}(n-\tfrac{1}{2}) \cosh\left[(n-\tfrac{1}{2})(\xi_{13}-\xi_{23})\right]$$
$$+ \tfrac{1}{2} D_n^{(2)}(n+\tfrac{3}{2}) \cosh\left[(n+\tfrac{3}{2})(\xi_{13}-\xi_{23})\right]$$
$$+ \tfrac{1}{2} E_n^{(2)}\{ (n-\tfrac{1}{2}) \sinh\left[(n-\tfrac{1}{2})(\xi_{13}-\xi_{23})\right] - (n+\tfrac{3}{2}) \sinh\left[(n+\tfrac{3}{2})(\xi_{13}-\xi_{23})\right]\}. \tag{A 11}$$

Here,

$$C_n^{(1)} = (M_n^{(1)} L_n^{(2)} - K_n^{(2)} N_n^{(1)})/\Delta_n, \tag{A 12}$$

$$C_n^{(2)} = (M_n^{(2)} L_n^{(2)} - K_n^{(2)} N_n^{(2)})/\Delta_n, \tag{A 13}$$

$$D_n^{(1)} = (K_n^{(1)} N_n^{(1)} - M_n^{(1)} L_n^{(1)})/\Delta_n, \tag{A 14}$$

$$D_n^{(2)} = (K_n^{(1)} N_n^{(2)} - M_n^{(2)} L_n^{(1)})/\Delta_n, \tag{A 15}$$

where

$$\Delta_n = K_n^{(1)} L_n^{(2)} - K_n^{(2)} L_n^{(1)}, \tag{A 16}$$

$$K_n^{(1)} = \frac{2\mu_3}{\mu_2} G_n^{(2)} - G_n^{(1)} (n - \tfrac{1}{2}), \tag{A 17}$$

$$K_n^{(2)} = \frac{2\mu_3}{\mu_2} G_n^{(3)} - G_n^{(1)} (n + \tfrac{3}{2}), \tag{A 18}$$

$$M_n^{(1)} = G_n^{(1)} F_n^{(1)}, \tag{A 19}$$

$$M_n^{(2)} = \frac{\mu_3}{\mu_2} \frac{n(n+1)}{\sqrt{2}} \left\{ \left[ -\frac{\mu_1}{\mu_2} (2n+1) + \frac{\mu_3}{\mu_2} (n - \tfrac{1}{2}) \right] e^{-(n+\frac{3}{2})\xi_{13}} \right.$$
$$\left. - \left[ -\frac{\mu_1}{\mu_2} (2n+1) + \frac{\mu_3}{\mu_2} (n + \tfrac{3}{2}) \right] e^{-(n+\frac{3}{2})\xi_{13}} \right\}, \tag{A 20}$$

$$L_n^{(1)} = 2\frac{\mu_3}{\mu_2} \sinh\left[(n - \tfrac{1}{2})(\xi_{13} - \xi_{23})\right] - (n - \tfrac{1}{2}) \{ \cosh\left[(n - \tfrac{1}{2})(\xi_{13} - \xi_{23})\right]$$
$$- \cosh\left[(n + \tfrac{3}{2})(\xi_{13} - \xi_{23})\right]\}. \tag{A 21}$$

$$L_n^{(2)} = 2\frac{\mu_3}{\mu_2} \sinh\left[(n + \tfrac{3}{2})(\xi_{13} - \xi_{23})\right] - (n + \tfrac{3}{2}) \{ \cosh\left[(n - \tfrac{1}{2})(\xi_{13} - \xi_{23})\right]$$
$$- \cosh\left[(n + \tfrac{3}{2})(\xi_{13} - \xi_{23})\right]\}, \tag{A 22}$$

$$N_n^{(1)} = \frac{n(n+1)}{\sqrt{2}} \left[ e^{-(n-\frac{1}{2})\xi_{23}} - e^{-(n+\frac{3}{2})\xi_{23}} \right] \{ \cosh\left[(n - \tfrac{1}{2})(\xi_{13} - \xi_{23})\right]$$
$$- \cosh\left[(n + \tfrac{3}{2})(\xi_{13} - \xi_{23})\right]\}, \tag{A 23}$$

and

$$N_n^{(2)} = \frac{\mu_3}{\mu_2} \frac{n(n+1)}{\sqrt{2}} \left[ \frac{e^{-(n-\frac{1}{2})\xi_{13}}}{n - \tfrac{1}{2}} - \frac{e^{-(n+\frac{3}{2})\xi_{13}}}{n + \tfrac{3}{2}} \right]. \tag{A 24}$$

The terms on the right-hand side of (A 17)–(A 19) are given by

$$F_n^{(1)} = \frac{n(n+1)}{\sqrt{2}} \{ e^{-(n-\frac{1}{2})\xi_{23}} - e^{-(n+\frac{3}{2})\xi_{23}} \}, \tag{A 26}$$

$$G_n^{(1)} = \frac{\mu_3}{\mu_2} \{ (n - \tfrac{1}{2})^2 \cosh\left[(n - \tfrac{1}{2})(\xi_{13} - \xi_{23})\right] - (n + \tfrac{3}{2})^2 \cosh\left[(n + \tfrac{3}{2})(\xi_{13} - \xi_{23})\right]\}$$
$$+ \frac{\mu_1}{\mu_2} (2n+1) \{ (n - \tfrac{1}{2}) \sinh\left[(n - \tfrac{1}{2})(\xi_{13} - \xi_{23})\right] - (n + \tfrac{3}{2}) \sinh\left[(n + \tfrac{3}{2})(\xi_{13} - \xi_{23})\right]\}.$$
$$\tag{A 27}$$

$$G_n^{(2)} = (n - \tfrac{1}{2}) \left\{ \frac{\mu_3}{\mu_2} (n - \tfrac{1}{2}) \sinh\left[(n - \tfrac{1}{2})(\xi_{13} - \xi_{23})\right] + \frac{\mu_1}{\mu_2} (2n+1) \cosh\left[(n - \tfrac{1}{2})(\xi_{13} - \xi_{23})\right] \right\},$$
$$\tag{A 28}$$

$$G_n^{(3)} = (n + \tfrac{3}{2}) \left\{ \frac{\mu_3}{\mu_2} \sinh\left[(n + \tfrac{3}{2})(\xi_{13} - \xi_{23})\right] + \frac{\mu_1}{\mu_2} (2n+1) \cosh\left[(n + \tfrac{3}{2})(\xi_{13} - \xi_{23})\right] \right\}. \tag{A 29}$$

## Appendix B

### *Drag-forces calculation*

With the flow field described by the stream functions in the form given by (2.31), (2.32) the drag force on each sphere can be obtained by following Stimson & Jeffery (1926). In particular, for the outer sphere we have

$$F_D = -\frac{\mu_2 \pi 2 \sqrt{2}}{c} \sum_{n-1}^{\infty} (2n+1)(A_n^{*(2)} + B_n^{*(2)} + C_n^{*(2)} + D_n^{*(2)}), \tag{B 1}$$

and for the inner sphere

$$f_D = -\frac{\mu_3 \pi 2 \sqrt{2}}{c} \sum_{n-1}^{\infty} (2n+1)(A_n^{*(3)} + B_n^{*(3)} + C_n^{*(3)} + D_n^{*(3)}). \tag{B 2}$$

By carrying our some lengthy algebra, the constants $A_n^{*(i)}$, $B_n^{*(i)}$, $C_n^{*(i)}$ and $D_n^{*(i)}$ can be related to $A_n$, $B_n$, $C_n$, $D_n$ and $E_n$, which are given by (A 1)–(A 29). By noting that these coefficients are linear in $U$ and $V$, it is clear that $f_D$ and $F_D$ exhibit a similar behaviour to that as given by (3.1–2). The coefficients $\alpha$, $\beta$, $\gamma$ and $\delta$ in (3.1) and (3.2) are given by

$$\alpha = \pi\mu_3 2 \sqrt{2} R_{23} \sinh \xi_{23} S_1, \tag{B 3}$$

$$\beta = \pi\mu_3 2 \sqrt{2} R_{23} \sinh \xi_{23} S_2, \tag{B 4}$$

$$\gamma = \pi\mu_2 2 \sqrt{2} R_{23} \sinh \xi_{23} S_3, \tag{B 5}$$

$$\delta = \pi\mu_2 2 \sqrt{2} R_{23} \sinh \xi_{23} S_4, \tag{B 6}$$

where

$$S_1 = \sum_{n=0}^{\infty} [(C_n^{(1)} + E_n^{(1)}) \, e^{-(n-\frac{1}{2})\xi_{23}} + (D_n^{(1)} - E_n^{(1)}) \, e^{-(n+\frac{3}{2})\xi_{23}}], \tag{B 7}$$

$$S_2 = \sum_{n=0}^{\infty} [(C_n^{(2)} + E_n^{(2)}) \, e^{-(n-\frac{1}{2})\xi_{23}} + (D_n^{(2)} - E_n^{(2)}) \, e^{-(n+\frac{3}{2})\xi_{23}}], \tag{B 8}$$

$$S_3 = \sum_{n=0}^{\infty} \left\{ -\frac{n(n+1)}{\sqrt{2}} \left[ \frac{e^{-(2n-1)\xi_{23}}}{n-\frac{1}{2}} - \frac{e^{-(2n+3)\xi_{23}}}{n+\frac{3}{2}} \right] + 2A_n^{(1)} \, [e^{-(n-\frac{1}{2})\xi_{23}} - e^{-(n+\frac{3}{2})\xi_{23}}] \right\}, \tag{B 9}$$

$$S_4 = \sum_{n=0}^{\infty} 2A_n^{(2)} \, [e^{-(n-\frac{1}{2})\xi_{23}} - e^{-(n+\frac{3}{2})\xi_{23}}]. \tag{B 10}$$

## REFERENCES

CHAMBERS, R. & KOPAC, M. J. 1937 The coalescence of living cells with oil drops. I. *Arbacia* eggs immersed in sea water. *J. Cell. Comp. Physiol.* 9, 331–343.

GOREN, S. L. & O'NEILL, M. E. 1971 On the hydrodynamic resistance to a particle of a dilute suspension when in the neighborhood of a large obstacle. *Chem. Engng Sci.* 26, 325–338.

HABER, S., HETSRONI, G. & SOLAN, A. 1973 On the low Reynolds number motion of two droplets. *Intl J. Multiphase Flow* 1, 57–71.

HAYAKAWA, T. & SHIGETA, M. 1974 Terminal velocity of two phase droplet. *J. Chem. Engng Japan* 7, 140–142.

JEFFERY, G. B. 1912 On a form of the solution of Laplace's equation suitable for problems relating to two spheres. *Proc. R. Soc. Lond.* A 87, 109–120.

JOHNSON, R. E. & SADHAL, S. S. 1983 Stokes flow past bubbles and drops partially coated with thin films. Part 2. Thin films with internal circulation – a perturbation solution. *J. Fluid Mech.* 132, 295–318.

JOHNSON, R. E. & SADHAL, S. S. 1985 Fluid mechanics of compound multiphase drops and bubbles. *Ann. Rev. Fluid Mech.* 17, 289–320.

KOPAC, M. J. & CHAMBERS, R. 1937 The coalescence of living cells with oil drops. II. *Arbacia* eggs immersed in acid or alkaline calcium solutions. *J. Cell. Comp.,Physiol.* **9**, 345–361.

LEE, S. H. & LEAL, L. G. 1980 Motion of a sphere in the presence of a plane interface. Part 2. An exact solution in bipolar coordinates. *J. Fluid Mech.* **98**, 193–224.

LI, N. N. & ASHER, W. J. 1973 Bllod oxygenation by liquid membrane permeation. In *Chem. Engng in Medicine*, Adv. Chem. Ser. **118**, 1–14.

MERCIER, J. L., DA CUNHA, F. M., TEIXEIRA, J. C. & SCOFIELD, M. P. 1974 Influence of enveloping water layer on the rise of air bubbles in Newtonian fluids. *Trans ASME* E: *J. Appl. Mech.* **96**, 29–34.

MEYYAPPAN, M., WILCOX, W. R. & SUBRAMANIAN, R. S. 1981 Thermocapillary migration of a bubble normal to a plane surface. *J. Colloid Interface Sci.* **83**, 199–208.

MORI, Y. H. 1978 Configurations of gas–liquid two-phase bubble in immiscible liquid media. *Intl J. Multiphase Flow* **4**, 383–396.

O'NEILL, M. E. 1964 A slow motion of a viscous fluid caused by a slowly moving solid sphere. *Mathematica* **11**, 67–74.

RASMUSSEN, R. M., LEVIZZANI, V. & PRUPPACHER, H. R. 1982 A numerical study of heat transfer through a fluid layer with recirculating flow between concentric and eccentric spheres. *Pure Appl. Geophys.* **120**, 702–720.

RUSHTON, E. & DAVIES, G. A. 1973 The slow unsteady unsettling of two fluid spheres along their line of centers. *Appl. Sci. Res.* **28**, 37–61.

RUSHTON, E. & DAVIES, G. A. 1978 The slow motion of two spherical particles along their line of centers. *Intl J. Multiphase Flow* **4**, 357–381.

RUSHTON, E. & DAVIES, G. A. 1983 Settling of encapsulated droplets at low Reynolds numbers. *Intl J. Multiphase Flow* **9**, 337–342.

SADHAL, S. S. 1983 A note on the thermocapillary migration of a bubble normal to a plane surface. *J. Colloid Interface Sci.* **95**, 283–285.

SELECKI, A. & GRADON, L. 1976 Equation of motion of an expanding vapour drop in an immiscible liquid medium. *Intl J. Heat Mass Transfer* **19**, 925–929.

SHANKAR, N., COLE, R. & SUBRAMANIAN, R. S. 1981 Thermocapillary migration of a fluid droplet inside a drop in a space laboratory. *Intl J. Multiphase Flow* **7**, 581–594.

SHANKAR, N. & SUBRAMANIAN, R. S. 1983 The slow axisymmetric thermocapillary migration of an eccentrically placed bubble inside a drop in zero gravity. *J. Colloid Interface Sci.* **94**, 258–275.

SIDEMAN, S. & MOALEM-MARON, D. 1982 Direct contact condensation. *Adv. Heat Transfer* **15**, 227–281.

STIMSON, M. & JEFFERY, G. B. 1926 The motion of two spheres in a viscous fluid. *Proc. R. Soc. Lond.* A **111**, 110–116.

TOCHITANI, Y., NAKAGAWA, T., MORI, Y. H. & KOMOTORI, K. 1977 Vaporization of single liquid drops in an immiscible liquid. Part II. Heat transfer characteristics. *Wärme- und Stoffübertragung* **10**, 71–79.

TORZA, S. & MASON, S. F. 1970 Three phase interaction in shear and electrical fields. *J. Colloid Interface Sci.* **33**, 67–83.